Observation of Two-Proton Radioactivity of ^{19}Mg by Tracking the Decay Products

I. Mukha,[1,*] K. Sümmerer,[2] L. Acosta,[3] M. A. G. Alvarez,[1] E. Casarejos,[4] A. Chatillon,[2] D. Cortina-Gil,[4] J. Espino,[1] A. Fomichev,[5] J. E. García-Ramos,[3] H. Geissel,[2] J. Gómez-Camacho,[1] L. Grigorenko,[5,6,2] J. Hoffmann,[2] O. Kiselev,[2,7] A. Korsheninnikov,[6] N. Kurz,[2] Yu. Litvinov,[2] I. Martel,[3] C. Nociforo,[2] W. Ott,[2] M. Pfutzner,[8] C. Rodríguez-Tajes,[4] E. Roeckl,[2] M. Stanoiu,[2,9] H. Weick,[2] and P. J. Woods[10]

[1]*Universidad de Sevilla, ES-41012 Seville, Spain*
[2]*Gesellschaft für Schwerionenforschung, D-64291 Darmstadt, Germany*
[3]*Universidad de Huelva, ES-21071 Huelva, Spain*
[4]*Universidade de Santiago de Compostela, ES-15782 Santiago de Compostela, Spain*
[5]*Joint Institute for Nuclear Research, RU-141980 Dubna, Russia*
[6]*RRC "Kurchatov Institute," RU-123184 Moscow, Russia*
[7]*Johannes Gutenberg Universität, D-55099 Mainz, Germany*
[8]*IEP, Warsaw University, PL-00681 Warszawa, Poland*
[9]*IFIN-HH, P.O. BOX MG-6, Bucharest, Romania*
[10]*University of Edinburgh, EH1 1HT Edinburgh, United Kingdom*
(Received 27 March 2007; published 29 October 2007)

We have observed the two-proton radioactivity of the previously unknown ^{19}Mg ground state by tracking the decay products in-flight. For the first time, the trajectories of the $2p$-decay products, ^{17}Ne $+ p + p$, have been measured by using tracking microstrip detectors which allowed us to reconstruct the $2p$-decay vertices and fragment correlations. The half-life of ^{19}Mg deduced from the measured vertex distribution is 4.0(15) ps in the system of ^{19}Mg. The Q value of the $2p$ decay of the ^{19}Mg ground state inferred from the measured $p - p - {}^{17}$Ne correlations is 0.75(5) MeV.

DOI: 10.1103/PhysRevLett.99.182501 PACS numbers: 23.50.+z, 21.10.Tg, 27.20.+n, 29.40.Gx

Two-proton ($2p$) radioactivity, a spontaneous decay of an atomic nucleus by the emission of two protons, is the most recently discovered nuclear disintegration mode. This phenomenon was predicted for a number of proton-rich isotopes that lie beyond the proton drip line [1]. The $2p$ radioactivity has first been reported for ^{45}Fe with a half-life ($T_{1/2}$) of about 4 ms, which is about 1000 times longer than the quasiclassical estimate of "di-proton" (or ^{2}He-cluster) emission [2,3]. Further observations of $2p$ radioactivity reported for ^{54}Zn [4] and ^{94m}Ag [5] have confirmed unexpectedly large $T_{1/2}$ values of $2p$ precursors. The recently developed first quantum-mechanical theory of $2p$ radioactivity which uses a three-body "core"$+ p + p$ model [6,7] interprets this observation as being due to a considerable influence of Coulomb and centrifugal barriers together with nuclear structure effects, and is able to predict the regular existence of long-lived $2p$ precursors.

Experiments aimed at finding such an exotic nuclear decay are generally based on implantation of the radioactive atoms and subsequent detection of their decay. For the first time in studies of radioactivity, we have performed an in-flight-decay experiment in which all fragments are tracked and the decay vertices as well as the angular correlations of the decay products are deduced from the measured trajectories. The ^{19}Mg ground state is a prospective candidate for the observation of $2p$ radioactivity by the in-flight method. The pioneering theoretical studies of the $2p$ decay of ^{19}Mg in the framework of a three-body model [8] predict its half-life from 0.5 to 60 ps and its decay energy from 0.55 to 0.85 MeV.

The in-flight $2p$-decay experiment suggested in Ref. [9] was discussed in detail in Refs. [8,10]. The experimental setup is shown in Fig. 1. The ^{19}Mg ground state can be produced in a knockout reaction from ^{20}Mg with the subsequent $2p$ decay populating ^{17}Ne $+ p + p$. If the directions of the decay products are measured precisely, the decay vertex can be found as the point of closest approach of three fragment trajectories. The half-life of ^{19}Mg can be derived by fitting the measured vertex distribution by exponential functions convoluted with the tracking detector resolution.

The experiment was performed by using a 591A MeV beam of ^{24}Mg with an intensity of 10^{9} s^{-1}, accelerated by the SIS facility at GSI, Darmstadt. The beam hit a primary

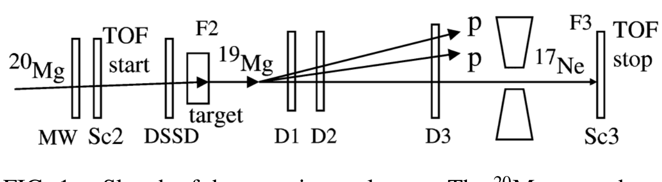

FIG. 1. Sketch of the experimental setup. The ^{20}Mg secondary beam was tracked by a silicon strip detector, DSSD, and a multiwire chamber, MW. ^{19}Mg nuclei were formed in the reaction (^{20}Mg, ^{19}Mg)X and products of the decays ^{19}Mg $\rightarrow$ ^{17}Ne $+ p + p$ were tracked by three planes of silicon microstrip detectors (D1–D3). ^{17}Ne ions were identified at foci F2 and F3 as described in the text.

4 g/cm^2 thick ^{9}Be target at the entrance of the Projectile-Fragment Separator (FRS) [11] to produce a 450A MeV secondary beam of ^{20}Mg with an average intensity of 400 ions s^{-1} at the midplane F2 of the FRS where the secondary reaction (^{20}Mg, ^{19}Mg) occurred in a second 2 g/cm^2 thick ^{9}Be target. Special magnetic optics settings were applied, the first half of the FRS being tuned in an achromatic mode using a wedge-shaped degrader, while its second half was set for identification of the heavy decay products with high acceptance in angle and momentum. A microstrip detector array [12], developed on the basis of the tracker of the AMS02 project [13], was positioned downstream of the secondary target. It consisted of four large-area (7×4 cm^2), 0.3 mm thick silicon microstrip detectors with a pitch of 0.1 mm. They measured energy loss and positions of coincident hits of two protons and ^{17}Ne, allowing one to reconstruct all fragment trajectories and derive the coordinates of the reaction vertex and angular proton-^{17}Ne correlations. The achieved transverse position accuracy is 40 μm for protons and 15 μm for ^{17}Ne. A 6×6 cm^2 double-sided Si strip detector (DSSD) with 32×32 strips and a 20×20 cm^2 multiwire chamber (MW) were used upstream of the target for tracking the ^{20}Mg projectiles. The heavy-ions like ^{17}Ne were unambiguously identified by their time of flight (TOF) between foci F2 and F3, their magnetic rigidity and their energy deposition measured with the position-sensitive scintillator detectors Sc2 and Sc3.

The $p - {}^{17}$Ne angular correlations carry information on the decay energy. As depicted in Fig. 2(a), the one-proton decay of a 1p-precursor leads to a characteristic angular correlation, with a peak appearing around the largest possible angle. Since the angles reflect the transverse proton momentum relative to ^{17}Ne, they are correlated with the decay energy. A similar effect is predicted by any calculation of direct 2p decay where the proton energy spectrum always has a relatively narrow peak centered close to half of the 2p-decay energy [8]. The measured angular correlations of protons with respect to ^{17}Ne, $\theta(p_1 - {}^{17}\mathrm{Ne}) - \theta(p_2 - {}^{17}\mathrm{Ne})$, are shown in Fig. 2(b). Most events fall into two distinct clusters: a spot around $\theta(p - {}^{17}\mathrm{Ne})$ of 30 mrad and a cross centered at 55 mrad. These two clusters may be attributed to the simultaneous 2p emission from the ^{19}Mg ground state and to the sequential decay of excited states in ^{19}Mg via the ^{18}Na ground state, respectively. We shall refer to these events as the "ground state" and "excited state," respectively.

A sketch of two ideal vertex profiles assuming a constant beam velocity across the target is shown in Fig. 3(a). The dissociation reaction of ^{20}Mg into the nonresonant ^{17}Ne + $p + p + n$ continuum should have a uniform distribution within the target. The same profile is expected if highly excited, short-lived states of ^{19}Mg are populated. The population of the ^{19}Mg ground state and its subsequent (delayed) radioactive decay is expected to exhibit "grow-

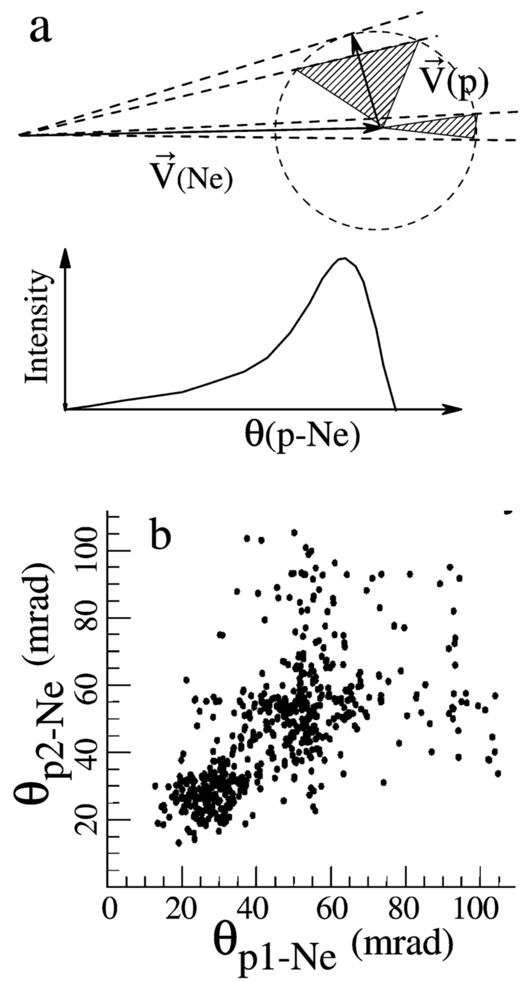

FIG. 2. (a) Illustration of the kinematical enhancement of angular correlations of decay products at the maximum possible angles between the decay products. (b) Angular $p - {}^{17}$Ne correlations obtained from the measured ^{17}Ne + $p + p$ events by selecting their vertex position inside the target (full circles).

in" and "decay" curves along the beam direction corresponding to radioactivity; this is analogous to counting decay products as a function of time in a standard radioactivity experiment. The vertex profile of the delayed emission is expected to be broader and shifted downstream in comparison with the profile of prompt 2p emission. Because of the limited spatial resolution of the detectors and angular straggling of the decay products both idealized profiles are smeared in reality.

Figures 3(b) and 3(c) show the experimental vertex profiles obtained from triple ^{17}Ne + $p + p$ events gated by the conditions of excited state and ground state groups from Fig. 2(b), respectively. These gates are inferred from the respective angular $p - {}^{17}$Ne correlations as discussed below in the context of Fig. 4. We have performed Monte Carlo simulations [14] of vertex profiles for the 2p-decay $^{19}\mathrm{Mg}^* \rightarrow {}^{17}\mathrm{Ne} + p + p$ shown in Fig. 3(b). The simulations assumed $T_{1/2} = 0$ for the excited states

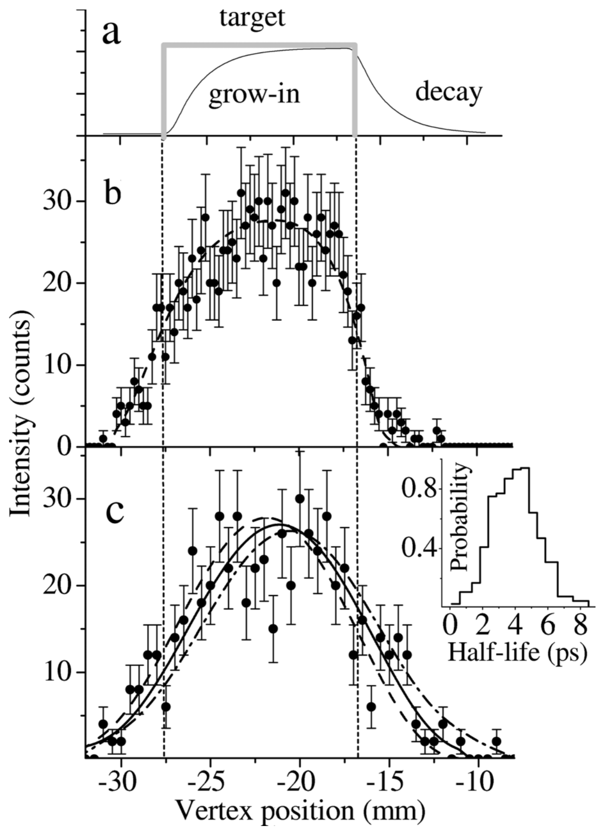

FIG. 3. Profiles of the reaction vertices along the beam direction with respect to the closest microstrip detector. (a) Ideal profiles of prompt (gray curve) and delayed (black curve) decays expected in a thick target. (b) Vertex distribution of ^{17}Ne + p + p events gated by large $p-{}^{17}$Ne angles (and thus large $p-{}^{17}$Ne relative energies), which corresponds to short-lived excited states in ^{19}Mg (full circles with statistical uncertainties). The dashed curve shows the Monte Carlo simulations of the detector response for the 2p-decay $^{19}\mathrm{Mg}^* \rightarrow {}^{17}\mathrm{Ne} + p + p$ with $T_{1/2} = 0$. (c) The same as (b) but gated by small $p-{}^{17}$Ne angles corresponding to the "ground state" group in Fig. 2(b). The dashed curve depicts a simulation of the 2p-decay component with $T_{1/2} = 0$. The solid and dash-dotted curves are fits to the data assuming a mixture of 25% of the $T_{1/2} = 0$ component and 75% of the radioactivity component with $T_{1/2}$ values of 4 and 8 ps, respectively. The inset shows the probability (as a function of the assumed half-lives) that the simulations match the data.

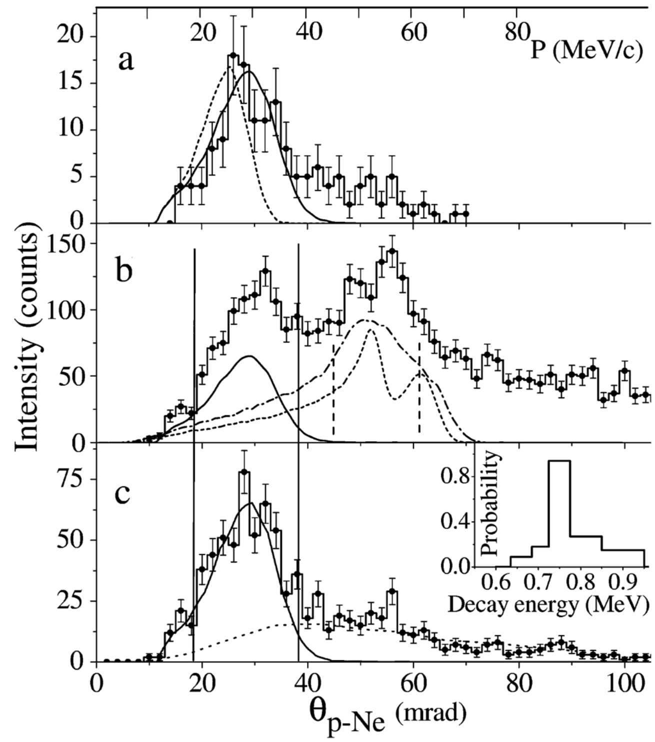

FIG. 4. Angular $p-{}^{17}$Ne correlations obtained from the measured ^{17}Ne + p + p events (histograms with statistical uncertainties) with three different gates: (a) events with vertex positions between the target and the first detector. The solid and dashed curves show the simulations for the model calculations [8] of the ^{19}Mg 2p decay with decay energies of 0.75 and 0.60 MeV, respectively. The upper axis shows the transverse proton momentum relative to ^{17}Ne. (b) Same as (a) but gated on a vertex inside the target. The solid curve is the same as in (a). The dashed and dash-dotted curves illustrate the sequential proton emission of a suggested excited state in ^{19}Mg via a narrow and a broad ($\Gamma = 0.5$ MeV) ground state of ^{18}Na, respectively. The vertical solid and dashed lines indicate the gates used for selecting vertex distributions for the "ground state" and "excited state" of ^{19}Mg, respectively (see text). (c) Angular $p_1-{}^{17}$Ne correlations selected in the same way as in (b) but additionally gated by a small angle in another $p_2-{}^{17}$Ne pair matching the ground state gate defined in (b). The solid curve is the same as in (a); the dotted curve is the fit of the broad distribution extrapolated into the ground state area. The inset shows the probability (as a function of 2p-decay energy) that the simulations match the data.

of ^{19}Mg and took into account the above-mentioned experimental position accuracies in tracking the fragments in reconstructing the decay vertex coordinates. The simulations reproduce the data with more than 90% probability, according to the standard statistical Kolmogorov test [15]. The small asymmetry of the rising and falling slopes of the vertices is due to multiple scattering of the fragments in the thick target. This vertex profile serves as the reference for estimating the position, width, and longitudinal uncertainty of the measured vertex distributions. The rms uncertainty of 0.8 mm has been derived from the falling slope of the vertex distribution in Fig. 3(b).

The vertex profile shown in Fig. 3(c) was accumulated under the condition that both protons originate from the ground state of ^{19}Mg. It has a broader distribution that is shifted in downstream direction by about 1 mm compared with the reference case displayed in Fig. 3(b). This shift unambiguously indicates a delayed activity. Its shape can be fitted by a simulation of the 2p radioactivity of ^{19}Mg by assuming $T_{1/2} = 3.1(10)$ ps. However, the observed vertex profile cannot be related to the 2p decay of the ^{19}Mg ground state alone. As will be discussed below, the events selected as representing the ground state decay actually contain contributions from both the ground state and excited states of this nucleus. Therefore, using the angular-correlation data discussed below, we have applied a two-component fit of the observed vertex profile shown in Fig. 3(c), with a mixture of 25% of the $T_{1/2} = 0$ component and 75% of the component with $T_{1/2} = 4.0(15)$ ps. The corresponding fit describes the data with about 95% probability. The uncertainty of this result is defined by the half-life range where the experimental data are described by the simulation with probability above 50%. The possible systematic uncertainty of $T_{1/2}$ due to the unknown shape of the $T_{1/2} = 0$ background is estimated by another fit of the $2p$-decay vertices gated by the condition that only one proton belongs to the ground state gate in Fig. 4(b). In this case the contribution of the $T_{1/2} = 0$ component is about 65%, and the derived $T_{1/2}$ value of ^{19}Mg amounts to $6(^{-2}_{-4})$ ps.

Figure 4 displays the angular $p - {}^{17}$Ne correlations derived from the coincident $^{17}\text{Ne} + p + p$ events. We made two projections from the measured $p - p - {}^{17}$Ne correlations. One was gated on vertices downstream of the target where the radioactivity of the ^{19}Mg ground state should show up [Fig. 4(a)]. The other distribution [Fig. 4(b)] was gated on vertices inside the target. The angular $p - {}^{17}$Ne correlations resulting from inside the target exhibit two peaks on top of a broad distribution while mostly one peak survives in the spectrum downstream from the target. The data are compared to simulations made for (i) the direct $2p$-decay $^{19}\text{Mg} \rightarrow {}^{17}\text{Ne} + p + p$ [8] and (ii) a sequential emission of protons from a suggested narrow state in ^{19}Mg via the ground state of ^{18}Na [16]. In both cases, the $2p$-decay energies were fitted to the peaks appearing in the experimental spectrum. The peak around 30 mrad was fitted by a Q_{2p} value of 0.75(5) MeV. In a similar way the peak around 55 mrad was fitted by assuming a sequential emission of 1.8 MeV protons from an excited state in ^{19}Mg to the ^{18}Na ground state and subsequently of 1.3 MeV protons, with a total Q_{2p} value of 3.2(2) MeV. Figure 4(c) shows the $p_1 - {}^{17}$Ne correlations corresponding to the ground state peak in another pair $p_2 - {}^{17}$Ne. The contribution from the ground state peak has the same shape as in Fig. 4(b), but the excited state peak is suppressed. This means that the ground state and excited state peaks cannot be explained by a sequential emission of protons from the same state in ^{19}Mg.

The derived Q_{2p} value of 0.75 MeV matches the range of $2p$-decay energies predicted for ^{19}Mg [8] while a $2p$-decay energy of about 3.2 MeV should result in immediate breakup regardless of the $2p$-decay mechanism involved. Therefore the only plausible explanation of the $p - {}^{17}$Ne correlations observed inside and outside the target is that the 55 mrad peak can be ascribed to an excited state in ^{19}Mg, and the 30 mrad peak is related to the ^{19}Mg ground state. In our procedure to determine the half-life of ^{19}Mg as described above, we have used these two peaks as gates for producing the $2p$-decay vertex distributions shown in Fig. 3. It should be noted that an unambiguous description of the 55 mrad excited state events is not possible due to lack of reliable knowledge about the ^{18}Na excited states [16].

Measurements of $2p$-decay energies and the vertices were calibrated by studying the known $2p$ decay of ^{16}Ne populated in the reaction (^{17}Ne, ^{16}Ne) with the ^{17}Ne secondary beam. The $p - {}^{14}$O angular correlations derived from $^{14}\text{O} + p + p$ triple coincidences yield a $2p$-decay energy matching the known value of 1.41(2) MeV [17]. For the falling slope of the longitudinal vertex profile of the $2p$ decays of ^{16}Ne, we obtained an rms value of 0.7 mm, in agreement with the ^{19}Mg excited state data.

To inspect alternative sources for the events ascribed to $2p$ emission, a vertex profile was produced by selecting ^{20}Mg as the heavy fragment in coincidence with two "protons," such events being presumably mimicked by δ electrons or detector noise. This background contributes less than 1% to the $^{17}\text{Ne} + p + p$ events of interest. No background contribution from $^{18}\text{Ne} + p + p$ events was observed either. The relative $^{17}\text{Ne} + p + p$ yield when ^{20}Mg breaks up into $^{18}\text{Ne} + p + p$ first and then ^{18}Ne loses one neutron within the thick target, thus imitating the delayed ^{19}Mg decay, is less than 0.1%. This estimate takes into account the ratio of 3 between ^{18}Ne and ^{17}Ne events detected at F3 and the cross section of 3 mb for $^{18}\text{Ne} \rightarrow {}^{17}\text{Ne} + n$ reactions obtained from the evaluation [18].

In summary, we report the observation of the ground state in ^{19}Mg and its $2p$ radioactivity. The delayed $2p$ emission is manifested in the measured decay vertex profile and in the $p - {}^{17}$Ne correlations. The ^{19}Mg vertex profile is shifted with respect to the target center, as expected for a short-lived radioactive nucleus. The $p - {}^{17}$Ne correlations display the ground and excited states of ^{19}Mg produced inside the target but only the ground state is seen outside the target in downstream direction. The measured half-life and decay energy match the predictions of the tree-body model while missing the predictions of the diproton model by 3 orders of magnitude [8]. The method of measuring radioactivity in-flight by precise tracking of all fragments with microstrip detectors has proven to be a promising tool for systematic studies of $2p$ emitters predicted theoretically [19].

The authors are indebted to M. Pohl and his co-workers of the DPNC, Universite de Génève, for developing the microstrip detectors. We appreciate, in particular, E. Cortina's continuous support of this project. We thank A. Bruenle, K. H. Behr, W. Hueller, A. Kelic, A. Kiseleva, R. Raabe and O. Tarasov for their help during the preparations of the experiment. This work has been supported by Contracts EURONS No. EC-I3 and No. FPA2003-05958 and No. FPA2006-13807-C02-01 (MEC, Spain).

*On leave from RRC "Kurchatov Institute," RU-123184 Moscow, Russia
mukha@us.es

[1] V. I. Goldansky, Nucl. Phys. **19**, 482 (1960).
[2] M. Pfutzner *et al.*, Eur. Phys. J. A **14**, 279 (2002).
[3] J. Giovinazzo *et al.*, Phys. Rev. Lett. **89**, 102501 (2002).
[4] B. Blank *et al.*, Phys. Rev. Lett. **94**, 232501 (2005).
[5] I. Mukha *et al.*, Nature (London) **439**, 298 (2006).
[6] L. V. Grigorenko *et al.*, Phys. Rev. Lett. **85**, 22 (2000).
[7] L. V. Grigorenko *et al.*, Phys. Rev. C **64**, 054002 (2001).
[8] L. V. Grigorenko, I. G. Mukha, and M. V. Zhukov, Nucl. Phys. **A713**, 372 (2003).
[9] I. Mukha and G. Schrieder, Nucl. Phys. **A690**, 280c (2001).
[10] I. Mukha, Phys. At. Nucl. **66**, 1519 (2003).
[11] H. Geissel *et al.*, Nucl. Instrum. Methods Phys. Res., Sect. B **70**, 286 (1992).
[12] http://dpnc.unige.ch/ams/GSItracker/www/.
[13] B. Alpat *et al.*, Nucl. Instrum. Methods Phys. Res., Sect. A **540**, 121 (2005).
[14] "GEANT—detector simulation tool," CERN software library, http://wwwinfo.cern.ch/asd/geant/.
[15] W. T. Eadie *et al.*, *Statistical Methods in Experimental Physics* (North-Holland, Amsterdam, 1971).
[16] T. Zerguerras *et al.*, Eur. Phys. J. A **20**, 389 (2004).
[17] C. J. Woodward, R. E. Tribble, and D. M. Tanner, Phys. Rev. C **27**, 27 (1983).
[18] K. Sümmerer and B. Blank, Phys. Rev. C **61**, 034607 (2000).
[19] L. V. Grigorenko, I. G. Mukha, and M. V. Zhukov, Nucl. Phys. **A714**, 425 (2003).